RSC Advances

PAPER

View Article Online
View Journal | View Issue

Cite this: *RSC Adv.*, 2014, **4**, 3201

Mg/N double doping strategy to fabricate extremely high luminescent carbon dots for bioimaging†

Fan Li,[a] Changjun Liu,*[a] Jian Yang,[a] Zheng Wang,[a] Wenguang Liu[b] and Feng Tian*[a]

Received 24th July 2013
Accepted 22nd October 2013

DOI: 10.1039/c3ra43826k

www.rsc.org/advances

Carbon dots (CDs) with quantum yield up to 83% have been synthesized with a Mg/N double doping fluorescence-enhanced strategy. Besides N-mediated surface passivation by ethylenediamine, the Mg–citric acid chelate played the roles of introducing Mg and preserving the carboxyl group, both greatly contributing to the photoluminescence enhancement of the final CDs. Importantly, the N- and Mg-doping functioned in concert without mutual influence.

Introduction

The surface-passivated carbonaceous quantum dots, so-called carbon dots (CDs), were discovered serendipitously by researchers purifying single-walled carbon nanotubes fabricated by arc-discharge methods.[1] Since then, CDs have been attracting considerable attention due to their versatile preparation routes, ready large scalability, better biocompatibility colloidal stability and particularly tunable photoluminescence (PL).[2–4] In the last decade, a variety of approaches have been explored for fabricating CDs, which can be generally classified into two main groups: top-down and bottom-up methods.[5] It has been confirmed by present reports that CDs can be produced inexpensively on a large scale for future practical applications through the "bottom-up" methods such as combustion/thermal[6–10] or microwave methods.[11–15] However, the treatment of CDs by strong acid or alkali was necessary to gain a strong fluorescent property in the early research.[16,17] Recently, some suitable molecular precursors with mild surface passivators or even without passivators are chosen to synthesize enhanced photoluminescent CDs using a one-step pathway.[9,18–20] In fact, all the CDs obtained from the "bottom-up" methods can be regarded as the products of incomplete carbonization of carbohydrate. Though some researchers have yet found the particle size of CDs is closely related to their fluorescence property,[21] it is now widely recognized that the surface state of CDs plays the key role in enhancing its fluorescence. So how to hold and enrich as much as possible specific chemical groups on the surface of CDs may be a facile way to enhance the PL.

Citric acid, a weak acid, has been reported to be used as carbon source to prepare CDs in which the surface passivation agent containing amino groups is necessary for yielding high PL.[19,20] Herein, we explore a simple route to prepare highly fluorescent CDs using citric acid as carbon source even without resorting to specialized surface passivation. It is well known that the metallic chelates possess preeminent thermal stability for their chelate rings similar to aromatic rings, and it has been proved that some functional groups such as amino and carboxyl groups[22] could be protected by chelating effect in the chemical reaction procedure. So the chelation of citric acid by divalent metal ions can protect the carboxyl groups of citric acid from over-consuming during the process of dehydration and carbonization. In this study, to prove our hypothesis, we chose magnesium hydroxide ($Mg(OH)_2$) as a representative chelation agent. To produce much higher PL CDs, Mg chelation in combination with nitrogen passivation, we called double doping strategy, will be attempted.

Experimental section

Chemicals and reagents

Citric acid (99%) and 3-(4,5-dimethyl-2-thiazoyl)-2,5-diphenyl tetrazolium bromide (MTT, 98%) were purchased from Alfa Aesar. Ethylenediamine (98%) and magnesium hydroxide (98%) were obtained from GuangFu Technology Development Co. Ltd. Quinine sulfate (98%, suitable for fluorescence) was supplied by Fluka. All other reagents were of analytical grades and used without further purification.

Preparation of high luminescent carbon dots

Typically, 10 g citric acid was dissolved in 40 mL distilled water followed by an adequate addition of 4.2 g $Mg(OH)_2$ in succession to form a colorless, transparent and homogeneous solution without other anions. Then a hydrothermal procedure was applied at 200 °C for 3 h. The raw products were treated with

[a]*Institute of Medical Equipment, Academy of Military Medical Sciences, Tianjin 300161, PR China. E-mail: hunterlcj@163.com; tianfeng62037@163.com*

[b]*School of Materials Science and Engineering, Tianjin Key Laboratory of Composite and Functional Materials, Tianjin University, Tianjin 300072, PR China*

† Electronic supplementary information (ESI) available: Experimental details and supplementary data. See DOI: 10.1039/c3ra43826k

further filtration, dialysis and lyophilization to obtain CDs denoted as Mg–CDs. Simultaneously, to gain a better understanding of the role of magnesium chelator in the formation of high fluorescent CDs, parallel experiments were also carried out as follows: (1) pyrolysis of citric acid without any doping, (2) using ethylenediamine (EDA) as surface passivation reagent without addition of $Mg(OH)_2$, and (3) with addition of both EDA and $Mg(OH)_2$. The corresponding resultant products were denoted as original CDs, EDA–CDs and Mg–EDA–CDs, respectively. More details were listed in the Table S1.†

Cell labeling and cytotoxicity assay

L929 cells were obtained from Peking Union Medical College (Beijing, China). The cells were cultured in medium of RPMI 1640 (1640, HyClone), containing 10% fetal bovine serum (FBS), 100 U mL^{-1} penicillin and 100 mg mL^{-1} streptomycin at 37 °C in 5% CO_2 humidified atmosphere.

For confocal microscope, L929 cells were seeded on a glass bottom culture dish (MatTek, USA) 12 h before use. Then the culture medium was replaced by 2.5 mL fresh medium containing 100 μg mL^{-1} CDs and the cells were incubated for another 24 h. The cells were washed with isotonic PBS (pH 7.4) three times. Then the L929 cells were fixed with 4% paraformaldehyde solution in PBS at 4 °C overnight. The samples were examined under a Leica confocal laser scanning microscope (Mannheim, Germany) equipped with a semiconductor laser (405 nm), an Ar laser (457/488/514 nm) and a HeNe laser (543/633 nm).

The cytotoxicity of CDs was assessed through MTT assay. L929 cells were seeded in a 96-well plate, at a density of 2×10^4 cells per well and incubated overnight. The following morning, the culture medium in each well was replaced by 180 μL fresh RPMI 1640/FBS. CDs solutions with various concentrations were then added to each well. After incubation for 24 h, the medium containing CDs was removed, and replaced with 200 μL fresh medium containing 20 μL MTT (5 mg mL^{-1} in PBS) and incubated for another 4 h. Finally all medium was removed and 150 μL per well dimethyl sulphoxide (DMSO) was added, followed by shaking for 15 min. The absorbance of each well at 490 nm was measured using a Synergy HT Multi-Mode Microplate Reader (BioTek, USA) with pure DMSO as a blank. Non-treated cells (in RPMI 1640) were used as a control and the relative cell viability (mean% ± SD, $n = 3$) was expressed as $Abs_{sample}/Abs_{control} \times 100\%$.

Measurements

UV-Vis absorption was measured on a TU-1810 UV-Vis spectrophotometer (Pgeneral, China). PL emission measurements were performed using FLS920 fluorometer (Edinburgh Instruments, Britain). The normalized spectrum was obtained by divided each intensity of the PL spectrum by the maximum value of its own. The morphology and microstructure of the CDs were examined by high-resolution transmission electron microscopy (HRTEM) on a Philips Tecnai G2 F20 microscope (Philips, Netherlands) with an accelerating voltage of 200 kV. The samples for HRTEM were made by dropping an aqueous solution onto a 300-mesh copper grid coated with a lacy carbon film. The Fourier transform infrared (FTIR) spectra of CDs were measured on a Nicolet 380 spectrometer (Thermo, USA). The surface states and composition of the samples were measured on a Kratos AXIS Ultra DLD X-ray Photoelectron Spectroscopy (XPS, Shimadzu, Japan). X-Ray diffraction (XRD) profiles of the prepared samples were recorded on a Rigaku-D/MAX 2500 diffractometer (Rigaku, Japan) equipped with graphite monochromatized CuKα ($\lambda = 0.15405$ nm) radiation at a scanning speed of 4° min^{-1} in the range from 5° to 60°.

Results and discussion

As one of the most important function indices, the quantum yield (QY) of CDs was measured at 360 nm excitation wavelength using quinine sulphate as a standard (QY = 54%). Remarkably, Mg–CDs exhibited a high QY value of 18.2% (Fig. S1†); while the QY of CDs without any doping was merely 0.8%. Amazingly, the QY of EDA–CDs reached 73.1%, which is close to the latest published results finished by Yang and his coworkers recently.[20] Importantly, the QY of Mg–EDA–CDs was further enhanced to as high as 83.0%, which is the highest value for CDs reported so far and almost equal to that of organic dyes or semiconductor quantum dots. Because of extremely high PL, blue fluorescent emission from aqueous solution of Mg–EDA–CDs could be easily observed under a UV lamp or even under a natural light (Fig. 1a).

The UV-Vis spectra of both EDA–CDs and Mg–EDA–CDs (Fig. S2†) showed obvious and similar absorption peaks centred at 346 nm ascribing to the n–π* transition, indicating the existence of aromatic structures in the CDs. As to Mg–EDA–CDs, a maximum PL emission peak was observed at around 437 nm when excited at 360 nm, closely near the position of UV-Vis absorption peak (Fig. 1a). However, we found a specific transition from primordial CDs to Mg–EDA–CDs in the PL emission spectra (Fig. 1b, $\lambda_{ex} = 360$ nm). The non-doped CDs showed a weaker peak at 459 nm compared with that of Mg–CDs at 437 nm. Likewise, EDA–CDs exhibited an emission peak at 449 nm in contrast with a 437 nm peak of Mg–EDA–CDs. The results revealed that an unknowable blue-shift phenomenon occurred to the CDs once doped with magnesium.

To further explore optical properties of the as-prepared CDs, we carried out a detailed PL study by changing excitation wavelengths ranging from 360 to 500 nm (Fig. 1c). With the increase of the excitation wavelength, the maximum emission peak position shifted to longer wavelength gradually but in a non-uniform mode, simultaneously accompanied with remarkable decrease of PL intensity. As different energy levels associated with different "surface states" formed by different functional groups are responsible for the excitation-dependent-emission phenomenon,[23] the observed excitation-dependent emission over 360–500 nm might be attributed to the relatively well-passivated but non-uniform CDs surface. The bathochromic shift phenomenon of emission from CDs has also been reported previously.[5,9,14,17]

Additionally, the influence of pH value on the PL intensity of the as-prepared CDs was also investigated (Fig. S8†). The PL intensity was very stable over the pH range of 3–11, which was favorable for CDs applications in the physiological and

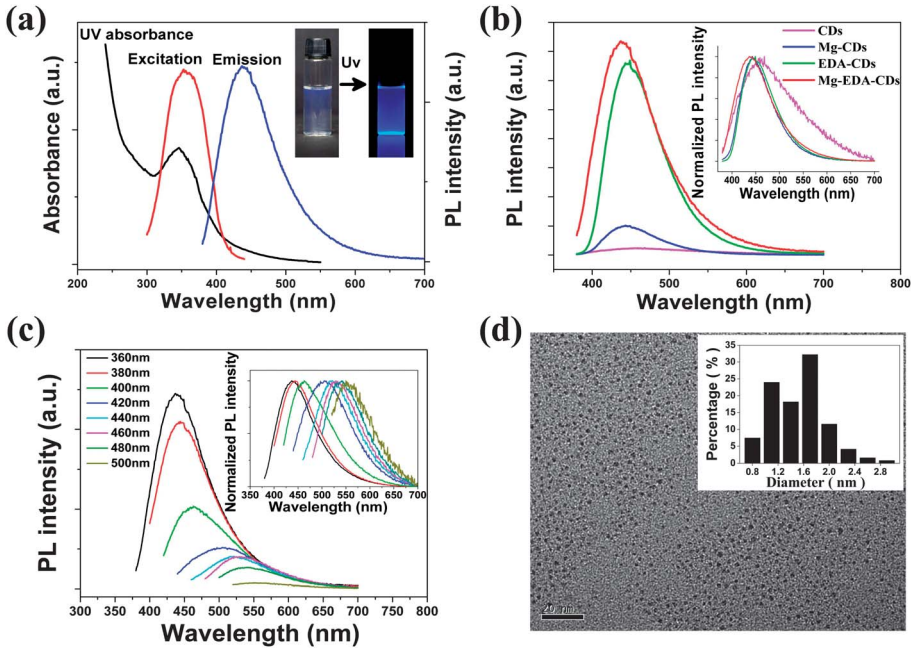

Fig. 1 (a) UV-Vis and PL spectra (λ_{ex} = 360 nm) of the Mg–EDA–CDs in aqueous solution (insets: photographs under natural light and UV light). (b) PL spectra (λ_{ex} = 360 nm) of CDs with different doping strategies. (c) PL emission spectra of Mg–EDA–CDs (insets of (b) and (c): the normalized PL emission spectra). (d) HRTEM image of Mg–EDA–CDs (scale bar: 20 nm).

pathological environments with a normal pH range of 4.5–9.5. And the PL intensity decreased slightly when the pH value was 1 or 13. This change was associated with the surface chemical groups of the CDs.[20]

HRTEM, XRD and FTIR spectra were conducted to characterize the micromorphology and chemical structure of CDs. The HRTEM images, as shown in Fig. 1d, displayed that Mg–EDA–CDs were well distributed among a narrow range between 0.8 and 2.8 nm without apparent agglomeration. From the magnified images (Fig. S3†), we can see, the overwhelming majority of CDs exhibited an amorphous structure; only a handful of CDs appeared barely distinguishable lattice fringes in the core area.[24] Owing to such a low carbon-lattice-structure content, the XRD patterns of the CDs (Mg–CDs, EDA–CDs, Mg–EDA–CDs, Fig. S4†) showed a very broad peak as a matter of course. Though the crystallization levels were related to carbonization degree somewhat, the CDs without any doping exhibited almost analogous particle size distribution and morphology (Fig. S5†) compared with Mg–EDA–CDs. Thus, it could be inferred that the great disparities in PL performances among these CDs probably stem from their different surface states and compositions.

It is commonly accepted that the fluorescence emission arises from the radiative recombination of the excitons trapped by the defects on the surface of CDs.[17,25–27] So to investigate the composition of CDs especially in the surface will help us to understand the PL mechanism. It was revealed by FTIR results (Fig. S6†) that Mg–CDs showed more obvious ν(C=O) peaks at 1617 cm^{-1} and ν(C–O) peaks at 1076 cm^{-1} compared with non-doped CDs. While EDA–CDs exhibited ν(N–H) peaks at 1555 cm^{-1} and ν(C–N) peaks at 1391 cm^{-1} indicating the successful anchoring of amino groups. Moreover, it is worthwhile to note that both Mg–CDs and Mg–EDA–CDs possess a similar and prominent peak at 1400 cm^{-1} ascribed to carboxylate anion (–COO$^-$). Further characterization studies using XPS

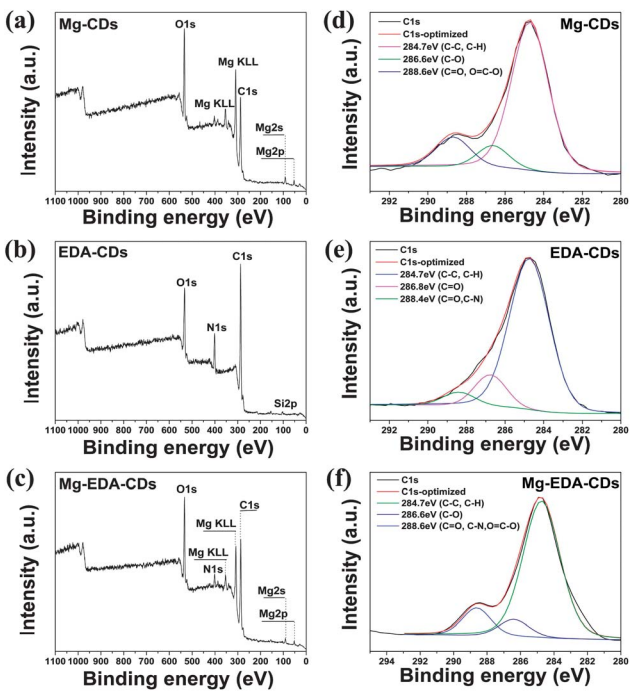

Fig. 2 XPS spectra of Mg–CDs (a), EDA–CDs (b) and Mg–EDA–CDs (c), XPS C 1s spectra of Mg–CDs (d), EDA–CDs (e) and Mg–EDA–CDs (f).

provided convincing evidence for the surface states and composition of the as-prepared CDs and the results were illustrated in Fig. 2. A 6.7% and 4.0% Mg atomic content were detected respectively from Mg–CDs and Mg–EDA–CDs, indicating the successful introduction of Mg into the CDs in an atomic state of Mg–CO_3 with a same binding energy at around 50 eV (shown in Fig. S7†). Moreover, their high-resolution C 1s spectra (Fig. 2d and f) showed strong signals at 288.6 eV attributing to the oxygenated carbon atoms (C═O, O═C–O) compared with that of EDA–CDs, which means more carboxyl groups fixed on the CDs surface. As to EDA–CDs and Mg–EDA–CDs, Fig. 2b and c reconfirmed a 10.9% and 4.5% N atomic content separately associated with N-doped surface passivation by EDA.[19]

The results obtained from above analyses demonstrate that the Mg–citric acid chelate in the carbon source plays dual roles in the hydrothermal process: introducing Mg and preserving the carboxyl group by chelation. Meanwhile, EDA functions as surface passivation reagent leading to doping N and amide–N contents. So, the Mg doping combined with N functionalization contributed to the great PL enhancement of CDs. Importantly, this double doping acted in concert without mutual interference.

The MTT assay method was used to evaluate the cytotoxicity of as-prepared Mg–EDA–CDs before applications and the results were demonstrated in Fig. S9.† The CDs exhibited low cytotoxicity with more than 90% cells retaining viability when incubated in the medium containing 250 μg mL^{-1} or lesser CDs. Thus an exploratory experiment was carried out to assess the potential application of CDs for cell imaging. L929 cells were cultured in the medium containing 100 μg mL^{-1} CDs for 24 h, washed with PBS three times, fixed with 4% paraformaldehyde solution in PBS at 4 °C overnight and then observed under a laser scanning confocal microscope. It is readily seen that CDs labeled L929 cells became bright excited at 405 nm, 488 nm and 543 nm, respectively, whereas the control cells (without CDs labeling, Fig. S10†) showed nearly no visible fluorescence detected under the same conditions. Meanwhile, based on Mg–EDA–CDs' specific emission characteristics (Fig. S11†) and fluorescence microscopy photographs of droplet containing CDs under bright field, ultraviolet (330–385 nm), blue (460–495 nm) and green (530–550 nm) light excitation (Fig. S12†), it could be reasonably inferred that CDs labeled L929 cells would show multicolor similar to Fig. 3 and S12† when excited at different wavelengths, which means more choices for us to observe CDs labeled samples. Furthermore, the CDs were observed mainly distributing over the cell membrane and the cytoplasmic area, while most cell nucleus showed very weak photoluminescence indicating there were little CDs. This result was consistent with the previous reports that CDs were able to label both the cell membrane and the cytoplasm but difficult to transport into the nucleus.[9,16] Together with no blink reconfirming the high photostability and the previous mentioned biocompatibility, Mg–EDA–CDs proved their great potential in biomedical fields.

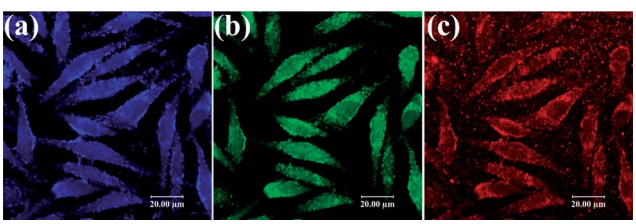

Fig. 3 Laser scanning confocal microscopy images of L929 cells labeled with CDs excited using 405 nm (a), 488 nm (b) and 543 nm (c) laser, and emission light was collected in the range of 432–490 nm, 516–551 nm and 595–657 nm, respectively. Scale bars: 20 μm.

Conclusion

In summary, we have explored a Mg/N double doping strategy to fabricate highly luminescent CDs. The Mg–citric acid chelate in the carbon source was utilized to introduce Mg and preserve more of carboxyl groups by chelation, which in conjunction with N passivation, contributed to a dramatic increase in the PL enhancement of the final CDs. Our work demonstrated that the resultant CDs are highly biocompatible and hold a great potential in biomedical applications.

Acknowledgements

The authors gratefully acknowledge the support for this work from the National Natural Science Foundation of China (Grant 51303210) and National Science and Technology Major Project of China (Grant 2012ZX10004801-003).

Notes and references

1 X. Y. Xu, R. Ray, Y. L. Gu, H. J. Ploehn, L. Gearheart, K. Raker and W. A. Scrivens, *J. Am. Chem. Soc.*, 2004, **126**, 12736.
2 S. T. Yang, L. Cao, P. G. Luo, F. Lu, X. Wang, H. Wang, M. J. Meziani, Y. Liu, G. Qi and Y. P. Sun, *J. Am. Chem. Soc.*, 2009, **131**, 11308.
3 F. Wang, Y. H. Chen, C. Y. Liu and D. G. Ma, *Chem. Commun.*, 2011, **47**, 3502.
4 Q. Li, T. Y. Ohulchanskyy, R. L. Liu, K. Koynov, D. Q. Wu, A. Best, R. Kumar, A. Bonoiu and P. N. Prasad, *J. Phys. Chem. C*, 2010, **114**, 12062.
5 S. N. Baker and G. A. Baker, *Angew. Chem., Int. Ed.*, 2010, **49**, 6726.
6 H. P. Liu, T. Ye and C. D. Mao, *Angew. Chem., Int. Ed.*, 2007, **46**, 6473.
7 L. Tian, D. Ghosh, W. Chen, S. Pradhan, X. Chang and S. Chen, *Chem. Mater.*, 2009, **21**, 2803.
8 Y. Q. Dong, N. N. Zhou, X. M. Lin, J. P. Lin, Y. U. Chi and G. Chen, *Chem. Mater.*, 2010, **22**, 5895.
9 Y. Yang, J. Cui, M. Zheng, C. Hu, S. Tan, Y. Xiao, Q. Yang and Y. Liu, *Chem. Commun.*, 2012, **48**, 380.
10 S. Zhu, J. Zhang, C. Qiao, S. Tang, Y. Li, W. Yuan, B. Li, L. Tian, F. Liu, R. Hu, H. Gao, H. Wei, H. Zhang, H. Sun and B. Yang, *Chem. Commun.*, 2011, **47**, 6858.
11 Q. L. Wang, H. Z. Zheng, Y. J. Long, L. Y. Zhang, M. Gao and W. J. Bai, *Carbon*, 2011, **49**, 3134.

12 A. Jaiswal, S. S. Ghosh and A. Chattopadhyay, *Chem. Commun.*, 2012, **48**, 407.
13 Z. Lin, W. Xue, H. Chen and J. M. Lin, *Chem. Commun.*, 2012, **48**, 1051.
14 C. Liu, P. Zhang, F. Tian, W. Li, F. Li and W. Liu, *J. Mater. Chem.*, 2011, **21**, 13163.
15 X. Wang, K. Qu, B. Xu, J. Ren and X. Qu, *J. Mater. Chem.*, 2011, **21**, 2445.
16 L. Cao, X. Wang, M. J. Meziani, F. S. Lu, H. F. Wang, P. J. G. Luo, Y. Lin, B. A. Harruff, L. M. Veca, D. Murray, S. Y. Xie and Y. P. Sun, *J. Am. Chem. Soc.*, 2007, **129**, 11318.
17 Y. P. Sun, B. Zhou, Y. Lin, W. Wang, K. A. S. Fernando, P. Pathak, M. J. Meziani, B. A. Harruff, X. Wang, H. F. Wang, P. J. G. Luo, H. Yang, M. E. Kose, B. L. Chen, L. M. Veca and S. Y. Xie, *J. Am. Chem. Soc.*, 2006, **128**, 7756.
18 S. F. Chin, S. N. A. M. Yazid, S. C. Pang and S. M. Ng, *Mater. Lett.*, 2012, **85**, 50.
19 X. Zhai, P. Zhang, C. Liu, T. Bai, W. Li, L. Dai and W. Liu, *Chem. Commun.*, 2012, **48**, 7955.
20 S. Zhu, Q. Meng, L. Wang, J. Zhang, Y. Song, H. Jin, K. Zhang, H. Sun, H. Wang and B. Yang, *Angew. Chem., Int. Ed.*, 2013, **14**, 3953.
21 F. Jiang, D. Chen, R. Li, Y. Wang, G. Zhang, S. Li, J. Zheng, N. Huang, Y. Gu, C. Wang and C. Shu, *Nanoscale*, 2013, **5**, 1137.
22 F. C. K. Chiu, R. T. C. Brownlee and D. R. Phillips, *Aust. J. Chem.*, 1993, **46**, 1207.
23 L. Tang, R. Ji, X. Cao, J. Lin, H. Jiang, X. Li, K. S. Teng, C. M. Luk, S. Zeng, J. Hao and S. P. Lau, *ACS Nano*, 2012, **6**, 5102.
24 J. Wang, C. Wang and S. Chen, *Angew. Chem., Int. Ed.*, 2012, **51**, 9297.
25 L. Y. Zheng, Y. W. Chi, Y. Q. Dong, J. P. Lin and B. B. Wang, *J. Am. Chem. Soc.*, 2009, **131**, 4564.
26 S. C. Ray, A. Saha, N. R. Jana and R. Sarkar, *J. Phys. Chem. C*, 2009, **113**, 18546.
27 B. R. Selvi, D. Jagadeesan, B. S. Suma, G. Nagashankar, M. Arif, K. Balasubramanyam, M. Eswaramoorthy and T. K. Kundu, *Nano Lett.*, 2008, **8**, 3182.